Derivation of low-temperature expansions for Ising model. VIII. Ferromagnetic and antiferromagnetic polynomials for the honeycomb-triangular system

1975 J. Phys. A: Math. Gen. 8 1448

(http://iopscience.iop.org/0305-4470/8/9/014)

J. Phys. A: Math. Gen., Vol. 8, No. 9, 1975. Printed in Great Britain.

Derivation of low-temperature expansions for Ising model VIII. Ferromagnetic and antiferromagnetic polynomials for the honeycomb–triangular system

M F Sykes, M G Watts and D S Gaunt

Wheatstone Physics Laboratory, King's College, Strand, London WC2R 2LS, UK

Received 9 May 1975

Abstract. The principle of partial code balance and the property of latent symmetry of the honeycomb–triangular code system are used to derive five new ferromagnetic polynomials ψ_{17} through ψ_{21} for both the triangular and honeycomb lattices. For the honeycomb lattice the corresponding antiferromagnetic polynomials though ψ^{A}_{21} are also derived.

1. Introduction

In this paper we study the derivation of ferromagnetic polynomials for the triangular lattice; the method used provides the corresponding partial codes and therefore an equivalent number of ferromagnetic and antiferromagnetic polynomials for the honeycomb lattice. We apply the general theory described in the previous papers of Sykes *et al* (1965, 1973a, b, c, d, e, 1975, to be referred to as I–VII), particularly II and VII; a general introduction and justification is given in VII.

We apply the techniques described in VII: the principle of partial balance and the property of latent symmetry. We also introduce the concept of a convex region which is fundamental to our treatment of the configurational problem.

In figure 1 we illustrate the configurations that contribute to the coefficient of u^9 for the triangular lattice, and which collectively constitute ψ_9. For such a small value of ω (the power of u) this example cannot be considered as typical, but already certain general features can be noticed. In particular the maximum power of μ (μ^7) corresponds to a configuration (number 1) with a strictly convex contour (defined precisely in § 2). The next highest power corresponds to three configurations, two (numbers 2 and 3) of which are strictly convex and one (number 4) is not; for this latter the concavity is limited to the presence of a re-entrant obtuse angle in the contour. Further examples of this type of concavity occur in μ^5. At μ^4 a more severe departure from strict convexity occurs in number 11 which exhibits two adjacent re-entrant obtuse angles. We describe terms not far removed from the strict convexity of numbers 1, 2 and 3 as *essentially convex*. In the region of ψ characterized by near maximum values of the power of μ, and for which configurations are strictly convex, many general results may be given. These results also hold when the configurations are not quite convex (essentially convex); the precise conditions which determine those concavities which are allowable depend on the property considered, some results requiring more stringent limitations than others; we use the term essentially convex to describe those configurations which may be treated as convex for a property under consideration. The length of the *convex region* in ψ,

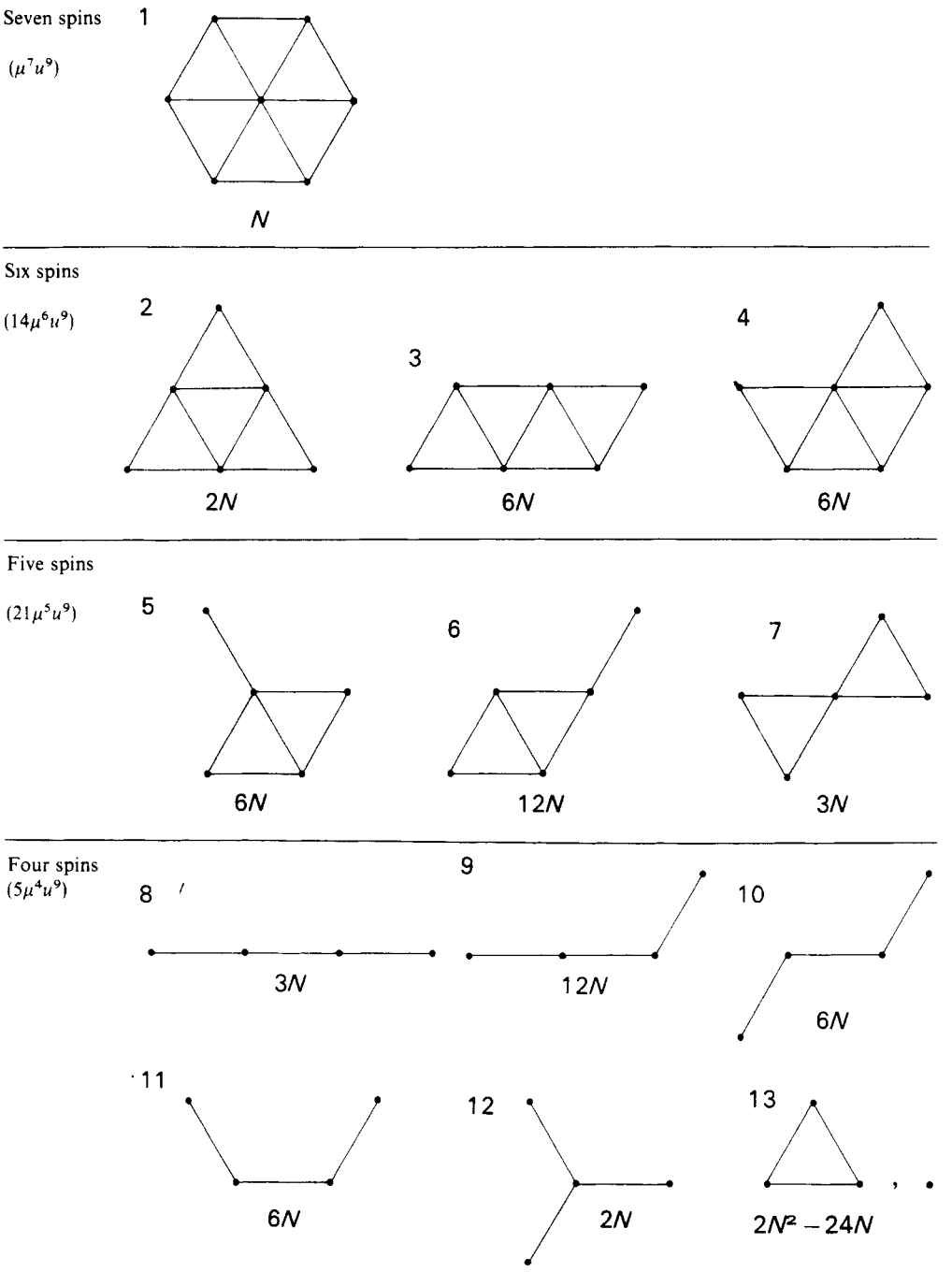

Figure 1. Configurational structure of ψ_9 on the triangular lattice.

that is the range of powers of μ throughout which the configurations may be treated as essentially convex, will vary from property to property. We elaborate on these ideas, and make them more precise, in § 2 where we examine certain geometrical properties of the triangular lattice.

As the power of μ decreases the connected configurations can exhibit more extreme departures from convexity and we enter the *concave region.* In μ^4 the separated configuration (number 13) has two components which are strictly convex; this illustrates a property we shall exploit: each time the number of components increases the individual components tend to be more convex than other configurations in the same region. In our example the ferromagnetic polynomial has a concave region, represented by μ^4. Finally ψ_9 terminates with a triplet of strictly convex components.

2. Geometrical properties

We now summarize certain elementary properties of the infinite triangular lattice which are more or less evident and find their origin deep in the literature of graph theory. We assume a general familiarity with the theory of duality (see, for example, Syozi 1972). We recall that for any perturbation of the ordered state the perturbed spins may be regarded as defining the interior of a closed graph conventionally drawn on the dual lattice (the honeycomb lattice), superimposed in the usual way. The length of this closed graph, measured by the total number of constituent edges, is the power of the temperature variable z and in our notation this power is represented by 2ω. We illustrate in figure 2

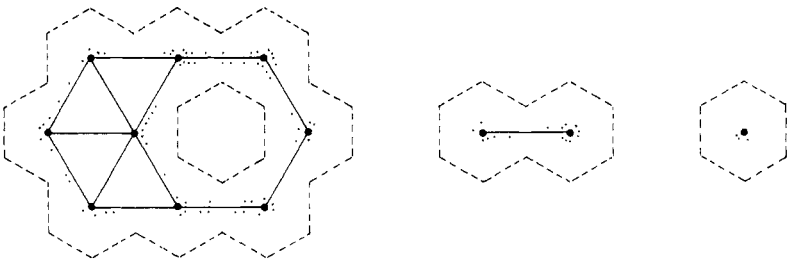

Figure 2. Example of a configuration on the triangular lattice with Ising perimeter $\omega = 22$. The contour (.....) is of length $\rho = 16$. The dual on the honeycomb lattice (------) has 44 edges.

a perturbation of 12 spins forming a three-component graph. One component has a *hole* in it (defined in VII, § 4). To define the *contour* suppose every elementary triangle of the lattice coloured A if it has three perturbed spins as its vertices, coloured B otherwise. Form a sum by assigning the value +1 to every bond in the configuration common to only one triangle of colour B, +2 to every bond common to two triangles of colour B, and zero otherwise. The total sum over all bonds we define as the length of the *contour* of the configuration. With this convention the first component of the graph in figure 2 contributes 14, the second 2, the third 0. The contour is represented geometrically by the closed curve on the dual shrunk or expanded towards the nearest perturbed spins. Denoting the length of the contour by ρ we have the elementary relation

$$\omega = \rho + 3c - 3h = \rho + 3\kappa \tag{2.1}$$

where κ is the discriminant of the configuration, a quantity we have already introduced in VII (equation (4.5)) and which also arises in the theory of the triplet model (Sykes and Watts 1975).

The closed curve delineated by the contour does not necessarily pass through all the perturbed spins. We call spins through which the contour passes *contour spins* and the remainder *internal spins*. The contour may pass through a spin once, twice or three times. Denoting the number of these three classes of contour spins by p_1, p_2, p_3 respectively, and the number of internal spins by p_0, we have the elementary relations

$$s = p_0 + p_1 + p_2 + p_3 \tag{2.2}$$

$$\rho = p_1 + 2p_2 + 3p_3. \tag{2.3}$$

We shall take it as evident without a formal demonstration that for the temperature or u-grouping for which ω (and therefore ρ) is fixed, the configurations with a near maximum number of spins correspond to contours for which $\kappa = 1$ and $p_2 = p_3 = 0$. In this latter case we have the result

$$s = p_0 + \rho$$

or

$$p_0 = s - \omega + 3 \tag{2.4}$$

$$(p_2 = p_3 = 0).$$

The ferromagnetic polynomials for the triangular lattice through ψ_{16} are given in IV. The general calculation was there based on an analysis of the *honeycomb* polygons which were used to deduce the terms corresponding to near maximum spin. The transformed linkage rule (2.1) in its contour form enables these terms to be re-classified as polygons on the *triangular* lattice. The maximum term always corresponds to an absolutely convex polygon and the general pattern of the convex end is found to conform to the scheme:

$$\begin{aligned}
\psi_{6m} &= \mu^{3m^2}(2 + 24\mu^{-1} + 128\mu^{-2} + \ldots \qquad m \gg 0 \\
\psi_{6m+1} &= \mu^{3m^2+m}(3 + 27\mu^{-1} + 147\mu^{-2} + \ldots \\
\psi_{6m+2} &= \mu^{3m^2+2m}(6 + 42\mu^{-1} + 198\mu^{-2} + \ldots \\
\psi_{6m+3} &= \mu^{3m^2+3m+1}(1 + 14\mu^{-1} + 87\mu^{-2} + \ldots \\
\psi_{6m+4} &= \mu^{3m^2+4m+1}(6 + 42\mu^{-1} + 198\mu^{-2} + \ldots \\
\psi_{6m+5} &= \mu^{3m^2+5m+2}(3 + 27\mu^{-1} + 147\mu^{-2} + \ldots .
\end{aligned} \tag{2.5}$$

From (2.5) and (2.2–3) it follows that for any $\psi_{3l}, \psi_{3l+1}, \psi_{3l+2}$ the number of coefficients in the region limited by the restriction $p_2 = p_3 = 0$ of (2.4) is $(l-1)$. For example in ψ_9 (figure 2), $l = 3$ and the configurations corresponding to $s = 7$ and $s = 6$ have no spins through which the contour passes more than once. The configurations at $s = 6$ are however still *connected* (one-component). It follows from (2.5) that the number of coefficients for which this connected property holds in any ψ_{2j}, ψ_{2j-1} is $j-2$; it suffices to consider a single isolated spin with the leading term of the ψ three places earlier in (2.5). The first *holes* appear as elementary hexagonal holes; if such a hole occurs in the coefficient of $u^\omega \mu^s$ then by placing a spin in it we obtain a configuration in $u^{\omega-3}\mu^{s+1}$ in contrast to a separated spin which if deleted yields a configuration in $u^{\omega-3}\mu^{s-1}$. The

onset of holes is therefore two coefficients after the onset of separated configurations. Denoting by $[x]$ the integer part of x we summarize these results:

In ψ_n

Length of region for which $p_2 = p_3 = 0$:	$[\frac{1}{3}n]-1$
Length of region without separated configuration:	$[\frac{1}{2}(n+1)]-2$
Length of region without holes:	$[\frac{1}{2}(n+1)]$.

(2.6)

Now we have shown in VII that in the region where all the graphs are connected the coefficients in ψ_n are determined completely by the principle of partial balance and patent symmetry; from (2.6) this implies that the last $[\frac{1}{2}(n+1)]-2$ coefficients are so determined. As the number of spins decreases the contours can become increasingly concave; however the first separated configurations will be essentially convex since they correspond to doublets whose components are selected from the convex end of earlier ψ. The same restrictions apply initially to holes: if the hole is removed by inserting a spin the resultant graph will be in the convex region of an earlier ψ. The number of holes is therefore calculable initially using (2.4), each interior point corresponding to one hole. The number of coefficients for which the contribution of holes ($\kappa = 0$) can be supplied in this way is limited by (2.6) applied to ψ_{n-3}. To add further coefficients it is also necessary to provide the separated configurations ($\kappa = 2$) and we describe a method of doing this in the next section.

3. Separated configurations in the convex region

The problem of calculating the number of strong embeddings of a multicomponent graph is one of classic difficulty. For the triangular lattice we have developed specialized techniques; a detailed treatment of the graph-theoretical background would require a long digression; since we are primarily concerned with the explicit derivation of ferromagnetic polynomials we shall only describe the general principles of the methods used and their practical application.

The problem of calculating the lattice constant of a two-component graph rests essentially on finding the number of embeddings of one component excluded by an embedding of the other. (Throughout the present section we shall treat different space-types of isomorphic graphs as distinct; this is not essential but avoids having to sum over all space-types at each stage.) Suppose G and G' are any two graphs (and as usual we denote their respective lattice constants by the same symbols): we can define their respective exclusions by writing the total number of embeddings of the (separated) two-component graph G, G':

$$NG(NG' - E(G', G)) = NG'(NG - E(G, G')) \tag{3.1}$$

where $E(G', G)$ is the number of embeddings of G' excluded by G. By symmetry $GE(G', G) = G'E(G, G')$. In general it is not possible to give an explicit expression for $E(G', G)$. The exception is in the convex region for which we quote, without proof, a graph-theoretic result.

Theorem

If G and G' are any two *absolutely convex* graphs on the triangular lattice with n, n' spins

and ω, ω' Ising perimeters (the powers of u) respectively, then

$$\frac{E(G', G)}{G'} = \frac{E(G, G')}{G} = \tfrac{1}{2} + (n + n') + \tfrac{1}{2}(\omega + \omega') + \tfrac{1}{6}\omega\omega'. \tag{3.2}$$

In the restricted enunciation above the theorem is of limited application; in fact it holds for many pairs of graphs which are *not* absolutely convex. We shall regard G as convex with respect to G' (and the converse) if the theorem holds for the separated graph $[G, G']$. Although there are many mutually convex pairs of graphs, including cases for which neither G nor G' is absolutely convex, the theorem fails if it is possible to form a *hole* (defined precisely in VII, § 4) by the superposition of some pair of embeddings of G and G' (the term superposition being defined as the strongly embedded graph whose vertex set is the union of the vertex sets of the respective embeddings of G and G').

If we particularize (3.2) to the case when G' is a single spin by substituting $s' = 1$, $\omega' = 3$ we obtain for the *spin exclusion* E_S of a convex graph

$$E_S = s + \omega + 3 \tag{3.3}$$

where s and ω refer to the excluding graph. As we move down the convex region of any ψ the application of (3.3) is first limited by the possibility of superpositions of the type:

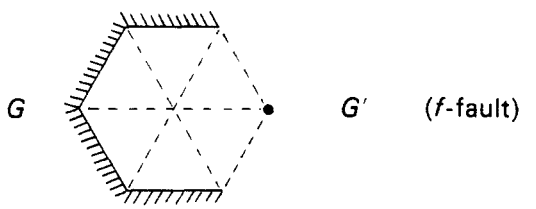

It can be proved that the validity of (3.3) is restored by assigning a weight of -1 to such superpositions. We denote the number of f-faults in G by f and write

$$E_S = s + \omega + 3 - f. \tag{3.4}$$

As we move further down ψ towards the concave region the possible faults that could give rise to a hole increase in complexity; faults also occur that can give rise to more than one hole. A superposition with h holes must be assigned a weight of $-h$. By a detailed classification of possible faults a practical working formula can be derived for the convex region. As a second example we substitute in (3.2) the parameters for the bond ($s' = 2$, $\omega' = 5$) and obtain for the bond exclusion E_B of a convex graph

$$E_B = 3s + 4\omega + 15. \tag{3.5}$$

The validity of this formula is restricted by more stringent limitations on the allowable departures from absolute convexity of G. The first fault to occur in ψ as we move down the convex region is of the type:

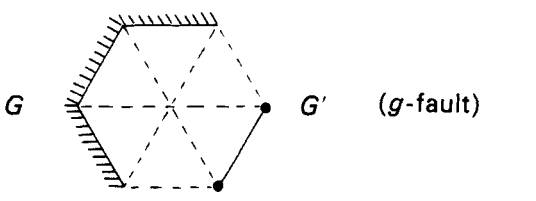

As before the validity of (3.5) is restored by assigning an extra weight of -1 to such superpositions. At the same time corrections can be made for f-faults by noticing that there are five embeddings of a bond that can give rise to a hole in the vicinity of an f-fault. The range of validity can be extended by writing

$$E_B = 3s + 4\omega + 15 - g - 5f. \tag{3.6}$$

If the theory is applied successively to all possible doublets G, G' in a *field* grouping ($n + n' =$ constant) the most difficult cases will correspond to $n \simeq n'$ and the corrections that must be made are very detailed. However, if the doublets are treated in the order they arise for the *temperature* grouping ($\omega + \omega' =$ constant) a simplification results; in general as the number of spins in G' increases, so G is more likely to be convex; this is a consequence of the geometrical properties described in § 2.

For example the polynomial ψ_{16} has six coefficients, μ^{21} down to μ^{16}, composed of only connected configurations; doublets appear in μ^{15} down to μ^{13} for which G' is a single spin ($\omega' = 3$) and therefore G corresponds to some graph in the coefficients of highest spin in ψ_{13}; at μ^{12} doublets for which G' is a bond ($\omega' = 5$) occur; at this point G corresponds to the terms of maximum power of μ in ψ_{11} for doublets with a bond, but four below maximum power of μ for doublets with a spin. Thus the bond will be first associated with strictly convex graphs at a point where the spin is already associated with graphs four displacements below the strictly convex region. The corrections required to (3.5) are therefore required later than those to (3.3) and this compensates for their greater complexity.

As a further application the result (3.2) can be used to count multicomponent graphs. By the general methods of Sykes *et al* (1966) any multicomponent graph may be made to depend (essentially, *mutatis mutandis*, by successive applications of Theorem 2, § 3) on the number of embeddings of two-component graphs. In general the calculation of a multicomponent graph $G, G', G'', \ldots$ will lead to doublets G, G^* for which G^* cannot be regarded as convex. For example if G^* has a concavity of the type represented by the f-fault there can be no graph G, even strictly convex, that does not admit of at least one superposition that contains a hole. Special procedures can be developed to overcome these difficulties in practice and useful working formulae derived. As an example of these we quote results for a triplet $[G, G', G'']$ and quadruplet $[G, G', G'', G''']$ when G', G'' and G''' are all single spins and G is *strictly* convex.

In an obvious notation

$$E_{S,S} = \tfrac{1}{2}(n^2 + 2n\omega + \omega^2 + 13n + 15\omega + 42) \tag{3.7}$$

$$E_{S,S,S} = -\tfrac{1}{6}(n^3 + 3n^2\omega + 3n\omega^2 + \omega^3 + 30n^2 + 66n\omega + 36\omega^2 + 305n + 383\omega + 1044). \tag{3.8}$$

These formulae will first be required as we move down ψ_n at the point where G is *strictly* convex, being in the maximum power of μ in ψ_{n-6} or ψ_{n-9} respectively. Departures from convexity can be allowed for by introducing the appropriate corrections; for example the correction to (3.7) for f- and g-faults is found to be

$$-\tfrac{1}{2}(2n + 2\omega + 17)f + \tfrac{1}{2}f^2 - g. \tag{3.9}$$

The derivation of all the formulae and corrections required for the present application is a long and detailed one. In practice we have avoided the necessity of calculating doublets by using latent symmetry and balance since at each stage these are the most numerous. We have used the methods outlined to calculate all the multicomponent graphs required to determine ψ through ψ_{21}. We have been able to calculate the 550

three-component and 17 four-component graphs that occur in the coefficient of μ^{12} in ψ_{21} and this represents the most extensive application we have made. We have made a further application of (3.3) to the problem of enumerating all the connected configurations by computer; it is a straightforward matter to count connected configurations with a fixed number of spins using the methods outlined by Martin (1974); the machine generation of configurations with a fixed contour can be achieved by imposing a restriction on the number of sites adjacent to each configuration. Since the corrections to (3.3) are all negative the number of adjacent sites cannot exceed $\omega+3$; by limiting this site perimeter to 24 we have generated all the connected partial codes through ψ_{21}.

4. General code pattern for temperature grouping

To determine the general code pattern appropriate for the temperature grouping or ψ_n we start with the algebraic code system defined by III (equation (2.1))

$$\begin{aligned}&(\lambda, \alpha, \beta, \gamma) = (3s-2C-j,\ 3s-3C-2j,\ j,\ C)\\ &\alpha \geqslant 0, \qquad \beta \geqslant 0, \qquad \gamma \geqslant 0.\end{aligned} \tag{4.1}$$

The problem is to find the number of algebraic codes in the coefficient of $\mu^s u^\omega$ which we denote by S_s^ω. It follows geometrically from the illustration of III (§ 2) that $\alpha \geqslant 3$ for any graphical code (a code for which at least one graph can be found on the shadow lattice). Further a code cannot be graphical if its image about the centre of symmetry in the even and odd regimes ((4.8) of VII) would imply another code with $\alpha < 0$ or $\beta < 0$ or $\gamma < 0$. A detailed examination of these restrictions yields the result

$$S_s^\omega = \begin{cases} \min(l, s-l+1) & \text{if } \omega = 3l \\ \min(l-1, s-l) & \text{if } \omega = 3l+1 \\ \min(l, s-l) & \text{if } \omega = 3l+2. \end{cases} \tag{4.2}$$

Since we are primarily concerned with the convex region (s large) these expansions may be simplified to

$$S_s^\omega = \begin{cases} l & \text{if } \omega = 3l \text{ or } 3l+2 \\ l-1 & \text{if } \omega = 3l+1 \end{cases} \tag{4.3}$$

Thus in the convex region the number of algebraic codes that need be considered is *independent of* s. In the concave region it follows from (4.2) that *fewer* codes need be considered than implied by (4.3). Any code is determined by three parameters but the condition that ω and s are constant reduces these to one. It is necessary to distinguish odd and even values of ω.

Odd regime (ω *odd*): In $\mu^s\mu^\omega$ there is a central code

$$(s+\tfrac{1}{2}\omega+\tfrac{1}{2},\ \tfrac{1}{2}\omega+1\tfrac{1}{2},\ \tfrac{1}{2}\omega-1\tfrac{1}{2},\ s-\tfrac{1}{2}\omega+\tfrac{1}{2}) \tag{4.4}$$

and denoting the number of displacements above this central code by λ the set of codes

will be

$$(s+\tfrac{1}{2}\omega+\tfrac{1}{2}+\lambda,\ \tfrac{1}{2}\omega+1\tfrac{1}{2}+3\lambda,\ \tfrac{1}{2}\omega-1\tfrac{1}{2}-3\lambda,\ s-\tfrac{1}{2}\omega+\tfrac{1}{2}+\lambda)$$
$$\lambda = 0,\ \pm 1,\ \pm 2\ldots \tag{4.5}$$

and the range of values of λ is limited by (4.3). For example at $\omega = 21$, $l = 7$ and $\lambda = 0$, ± 1, ± 2, ± 3.

Even regime (ω *even*): In $\mu^s\mu^{\omega}$ there are two central codes. Those above the centre of symmetry are given in ascending order of class by

$$(s+\tfrac{1}{2}\omega+\lambda,\ \tfrac{1}{2}\omega+3\lambda,\ \tfrac{1}{2}\omega-3\lambda,\ s-\tfrac{1}{2}\omega+\lambda)$$
$$\lambda = 1, 2, 3\ldots. \tag{4.6}$$

and those below in descending order by

$$(s+\tfrac{1}{2}\omega+1+\lambda,\ \tfrac{1}{2}\omega+3+3\lambda,\ \tfrac{1}{2}\omega-3-3\lambda,\ s-\tfrac{1}{2}\omega+1+\lambda)$$
$$\lambda = -1, -2, -3\ldots \tag{4.7}$$

with the range of values of λ limited by (4.3). For example at $\omega = 20$, $l = 6$ and $\lambda = 1, 2, 3$, in (4.6) and -1, -2, -3, in (4.7).

We illustrate in figures 3(*a*) and 3(*b*) grids of the code patterns corresponding to ψ_{21} and ψ_{20} respectively. We have shown in VII (§§ 3 and 4) that in the region where all the shadow graphs are connected ($\kappa = 1$) the code system is completely determined by successive applications of the principle of partial balance and patent symmetry. By

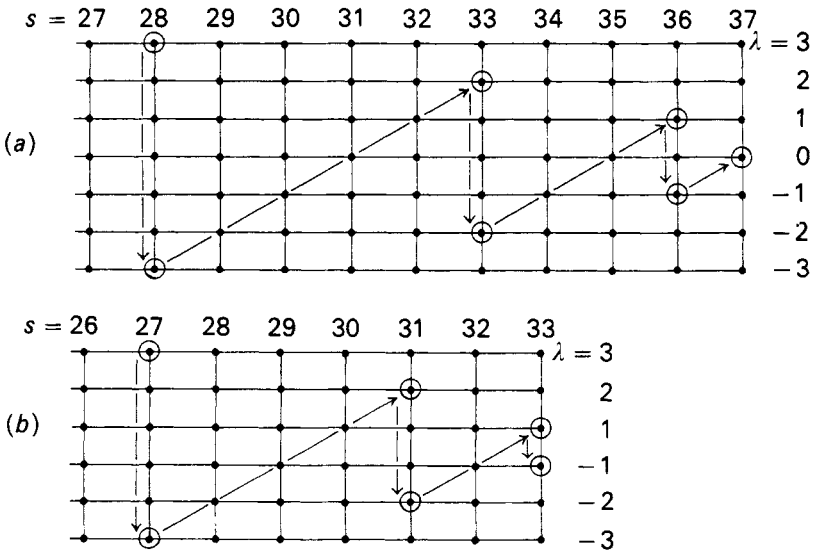

Figure 3. (*a*) Grid of codes in $\psi_{21}(\mu)$ illustrating the transmission of information (odd regime). •, algebraic code, ◉, related sequence of codes. Vertical arrows correspond to an application of patent symmetry, inclined arrows to an application of the principle of partial balance. (*b*) Grid of codes in $\psi_{20}(\mu)$ illustrating the transmission of information (even regime).

detailed examination the path taken by information can be traced backwards from any code. In the odd regime there is one central code of class $s-\frac{1}{2}\omega+\frac{1}{2}$ (a secondary code) which is determined by balance and the only code required that lies in ψ_ω is the code of class $s-\frac{1}{2}\omega-1\frac{1}{2}$ in μ^{s-1} (one below centre); this is a primary code but is determined by symmetry from the secondary code one above centre. The next code above centre is of class $s-\frac{1}{2}\omega+1\frac{1}{2}$ and the only code in ψ_ω required to complete it by partial balance is the primary code of class $s-\frac{1}{2}\omega-4\frac{1}{2}$ (two below centre) in μ^{s-3}. The next code above centre of class $s-\frac{1}{2}\omega+2\frac{1}{2}$ requires the code of class $s-\frac{1}{2}\omega-7\frac{1}{2}$ in μ^{s-5} (three below centre) and so on.

In the even regime the central code above centre of class $s-\frac{1}{2}\omega+1$ requires the code of class $s-\frac{1}{2}\omega-4$ in μ^{s-2} (two below centre). The next code above centre of class $s-\frac{1}{2}\omega+2$ requires the code of class $s-\frac{1}{2}\omega-6$ in μ^{s-4} (three below centre) and so on.

By applying the results to the grid of figure 3, it is found that the coefficient of any code can be traced back by ever increasing steps in s and at each stage λ increases by unity. But the grid width is *finite*. It follows that eventually the code required in ψ_ω falls outside the grid and is therefore *zero*. This implies that all the information is supplied by the ψ through $\psi_{\omega-1}$. In the convex region of patent symmetry the polynomial may be filled in completely from the previous ψ. At the point where the symmetry becomes latent new information must be supplied for chosen values of the discriminant to restore the symmetry of the code pattern.

5. Explicit extension of the temperature grouping

To extend the temperature grouping on the triangular lattice and derive ferromagnetic polynomials we have combined the three techniques described in preceding sections and in VII: partial balance, latent symmetry and the special properties of the convex region. To complete the convex end of the polynomials by balance we have restored the symmetry of the code patterns by providing the contribution corresponding to connected configurations by computer enumeration and the contributions corresponding to configurations with three or more components by the general methods of § 3; the contributions from configurations with a discriminant of two (doublets) then follow algebraically by the methods of § 4.

We have determined all the partial codes F_n^ω for the triangular lattice for all n through $\omega = 21$. These provide all the sublattice polynomials (II, § 1 and equation (1.7)) for the honeycomb lattice. The partial codes and sublattice polynomials are too extensive to be quoted in full. We give in the appendix the ferromagnetic polynomials $\psi_{17}, \psi_{18}, \psi_{19}, \psi_{20}, \psi_{21}$ for the triangular and honeycomb lattices. For these the values of ψ_n ($\mu = 1$) and $\partial\psi_n/\partial\mu$ ($\mu = 1$) are in agreement with the exact solution for the zero-field partition function and the spontaneous magnetization. The corresponding ferromagnetic susceptibility can be extended by five coefficients in each case to continue IV, equations (3.3) and (3.4):

$$\chi_T^f = \ldots + 50\,369\,760u^{17} + 56\,095\,776u^{18} + 484\,296\,732u^{19} + 571\,273\,344u^{20} + 4\,628\,107\,216u^{21} + \ldots \tag{5.1}$$

$$\chi_{HC}^f = \ldots + 2\,154\,378\,816z^{17} + 8\,395\,571\,712z^{18} + 32\,639\,750\,676z^{19} + 126\,625\,222\,200z^{20} + 490\,300\,659\,692z^{21} + \ldots. \tag{5.2}$$

The partial codes determine five new antiferromagnetic polynomials to supplement I (appendix 5), and IV (equation (3.6)):

$$\begin{aligned}
2\psi^{a}_{17} &= 286\,617\theta_1 + 46\,143\theta_3 + 576\theta_5 \\
2\psi^{a}_{18} &= 1\,080\,641\tfrac{1}{3} + 469\,318\theta_2 + 30\,488\theta_4 + 72\tfrac{2}{3}\theta_6 \\
2\psi^{a}_{19} &= 2\,729\,889\theta_1 + 536\,388\theta_3 + 12\,960\theta_5 \\
2\psi^{a}_{20} &= 10\,297\,044\tfrac{3}{5} + 4\,850\,139\theta_2 + 430\,149\tfrac{3}{4}\theta_4 + 3\,216\theta_6 \\
2\psi^{a}_{21} &= 27\,003\,275\theta_1 + 6\,216\,111\theta_3 + 238\,111\theta_5 + 355\tfrac{1}{7}\theta_7
\end{aligned} \tag{5.3}$$

and from these, or from (5.1) and (5.2) using II (4.22), the corresponding antiferromagnetic susceptibility can be extended by five coefficients to continue IV, equation (3.5):

$$\begin{aligned}
\chi^{a}_{HC} = \ldots &+ 2\,865\,216y^{17} + 9\,470\,784y^{18} + 31\,525\,524y^{19} + 105\,594\,912y^{20} \\
&+ 355\,673\,804y^{21} + \ldots .
\end{aligned} \tag{5.4}$$

Acknowledgment

This work has been supported through a Research Grant from the Science Research Council.

Appendix

Ferromagnetic polynomials $\psi(\mu)$ (for earlier terms see appendix to IV†).

Triangular lattice

$$\begin{aligned}
\psi_{17} = {} & 3\mu^{24} + 27\mu^{23} + 147\mu^{22} + 507\mu^{21} + 1\,401\mu^{20} + 2\,943\mu^{19} + 5\,412\mu^{18} + 8\,679\mu^{17} \\
& + 11\,784\mu^{16} + 13\,419\mu^{15} + 11\,103\mu^{14} + 6\,741\mu^{13} - 9\,036\mu^{12} - 21\,621\mu^{11} \\
& - 42\,315\mu^{10} - 11\,109\mu^{9} + 30\,825\mu^{8} + 63\,870\mu^{7} + 27\,555\mu^{6} \\
\psi_{18} = {} & 2\mu^{27} + 24\mu^{26} + 128\mu^{25} + 496\mu^{24} + 1\,458\mu^{23} + 3\,424\mu^{22} + 6\,936\mu^{21} + 11\,969\mu^{20} \\
& + 19\,168\mu^{19} + 26\,038\mu^{18} + 31\,090\mu^{17} + 29\,877\mu^{16} + 23\,046\mu^{15} + 2\,130\tfrac{1}{2}\mu^{14} \\
& - 30\,902\mu^{13} - 65\,829\mu^{12} - 111\,460\mu^{11} - 48\,618\tfrac{1}{2}\mu^{10} + 43\,868\tfrac{2}{3}\mu^{9} \\
& + 165\,894\tfrac{1}{2}\mu^{8} - 307\,476\mu^{7} - 7\,796\tfrac{2}{5}\mu^{6} \\
\psi_{19} = {} & 3\mu^{30} + 27\mu^{29} + 147\mu^{28} + 579\mu^{27} + 1\,719\mu^{26} + 4\,338\mu^{25} + 9\,138\mu^{24} + 17\,115\mu^{23} \\
& + 28\,809\mu^{22} + 43\,893\mu^{21} + 60\,543\mu^{20} + 71\,820\mu^{19} + 77\,325\mu^{18} \\
& + 64\,830\mu^{17} + 38\,946\mu^{16} - 25\,359\mu^{15} - 80\,940\mu^{14} - 195\,312\mu^{13} \\
& - 224\,955\mu^{12} - 136\,956\mu^{11} + 205\,386\mu^{10} + 375\,483\mu^{9} - 58\,668\mu^{8} \\
& + 437\,997\mu^{7}
\end{aligned}$$

† The coefficient of μ^8 in ψ_{16} for the honeycomb lattice is there printed with incorrect sign and should read $-74\,083\tfrac{7}{8}\mu^8$ in agreement with L_8 given in I (appendix).

$$\psi_{20} = 6\mu^{33} + 42\mu^{32} + 216\mu^{31} + 798\mu^{30} + 2\,412\mu^{29} + 6\,060\mu^{28} + 13\,128\mu^{27} + 25\,626\mu^{26}$$
$$+ 44\,514\mu^{25} + 72\,105\mu^{24} + 105\,816\mu^{23} + 142\,956\mu^{22} + 171\,300\mu^{21}$$
$$+ 187\,158\mu^{20} + 175\,416\mu^{19} + 120\,099\mu^{18} + 23\,730\mu^{17} - 123\,552\mu^{16}$$
$$- 288\,768\mu^{15} - 563\,163\mu^{14} - 549\,690\mu^{13} - 466\,116\mu^{12} + 473\,976\mu^{11}$$
$$+ 663\,288\mu^{10} + 408\,072\mu^{9} - 1\,907\,846\tfrac{1}{4}\mu^{8} - 275\,184\mu^{7}$$

$$\psi_{21} = \mu^{37} + 14\mu^{36} + 87\mu^{35} + 392\mu^{34} + 1\,341\mu^{33} + 3\,918\mu^{32} + 9\,632\mu^{31} + 21\,083\mu^{30}$$
$$+ 41\,040\mu^{29} + 73\,578\mu^{28} + 121\,804\mu^{27} + 186\,235\mu^{26} + 266\,341\mu^{25}$$
$$+ 347\,250\mu^{24} + 420\,677\mu^{23} + 456\,575\mu^{22} + 456\,246\mu^{21} + 345\,275\mu^{20}$$
$$+ 177\,611\mu^{19} - 110\,316\mu^{18} - 440\,030\mu^{17} - 961\,349\mu^{16} - 1\,312\,194\mu^{15}$$
$$- 1\,423\,670\mu^{14} - 779\,285\mu^{13} + 1\,264\,848\mu^{12} + 2\,435\,614\mu^{11} + 1\,680\,030\mu^{10}$$
$$- 3\,019\,394\mu^{9} + 4\,905\,025\mu^{8} + 65\,718\tfrac{1}{7}\mu^{7}$$

Honeycomb Lattice

$$\psi_{17} = 3\mu^{47} + 21\mu^{45} + 108\mu^{43} + 423\mu^{41} + 1\,422\mu^{39} + 4\,170\mu^{37} + 10\,899\mu^{35} + 25\,782\mu^{33}$$
$$+ 55\,107\mu^{31} + 106\,380\mu^{29} + 184\,413\mu^{27} + 279\,855\mu^{25} + 357\,888\mu^{23}$$
$$+ 341\,706\mu^{21} + 103\,503\mu^{19} - 438\,600\mu^{17} - 1\,045\,935\mu^{15} - 711\,801\mu^{13}$$
$$+ 1\,409\,742\mu^{11} - 367\,878\mu^{9} + 16\,128\mu^{7}$$

$$\psi_{18} = \tfrac{1}{2}\mu^{54} + 7\mu^{52} + 43\tfrac{1}{2}\mu^{50} + 196\mu^{48} + 721\tfrac{1}{2}\mu^{46} + 2\,316\mu^{44} + 6\,595\mu^{42} + 17\,039\tfrac{1}{2}\mu^{40}$$
$$+ 40\,208\mu^{38} + 87\,091\mu^{36} + 173\,843\tfrac{1}{2}\mu^{34} + 317\,845\mu^{32} + 529\,286\tfrac{1}{2}\mu^{30}$$
$$+ 792\,105\mu^{28} + 1\,028\,767\tfrac{1}{2}\mu^{26} + 1\,085\,059\tfrac{1}{2}\mu^{24} + 708\,809\tfrac{1}{2}\mu^{22}$$
$$- 398\,467\tfrac{1}{2}\mu^{20} - 2\,171\,765\tfrac{1}{3}\mu^{18} - 3\,392\,069\mu^{16} - 1\,106\,330\tfrac{1}{2}\mu^{14}$$
$$+ 4\,905\,536\tfrac{5}{6}\mu^{12} - 1\,706\,988\tfrac{1}{2}\mu^{10} + 120\,844\mu^{8} - 495\tfrac{1}{6}\mu^{6}$$

$$\psi_{19} = 3\mu^{59} + 21\mu^{57} + 108\mu^{55} + 429\mu^{53} + 1\,467\mu^{51} + 4\,431\mu^{49} + 12\,114\mu^{47} + 30\,420\mu^{45}$$
$$+ 70\,545\mu^{43} + 152\,220\mu^{41} + 305\,637\mu^{39} + 571\,479\mu^{37} + 992\,772\mu^{35}$$
$$+ 1\,588\,965\mu^{33} + 2\,318\,640\mu^{31} + 3\,018\,270\mu^{29} + 3\,324\,459\mu^{27}$$
$$+ 2\,706\,057\mu^{25} + 487\,428\mu^{23} - 3\,777\,609\mu^{21} - 8\,836\,677\mu^{19} - 9\,879\,492\mu^{17}$$
$$+ 589\,338\mu^{15} + 16\,327\,032\mu^{13} - 7\,495\,464\mu^{11} + 776\,475\mu^{9} - 9\,831\mu^{7}$$

$$\psi_{20} = 1\tfrac{1}{2}\mu^{66} + 13\tfrac{1}{2}\mu^{64} + 73\tfrac{1}{2}\mu^{62} + 310\tfrac{1}{2}\mu^{60} + 1\,099\tfrac{1}{2}\mu^{58} + 3\,447\mu^{56} + 9\,771\mu^{54} + 25\,446\mu^{52}$$
$$+ 61\,500\mu^{50} + 138\,888\mu^{48} + 294\,511\tfrac{1}{2}\mu^{46} + 586\,908\mu^{44} + 1\,101\,562\tfrac{1}{2}\mu^{42}$$
$$+ 1\,942\,245\mu^{40} + 3\,209\,931\mu^{38} + 4\,944\,511\tfrac{1}{2}\mu^{36} + 7\,017\,771\mu^{34}$$
$$+ 9\,029\,640\tfrac{3}{4}\mu^{32} + 10\,163\,883\mu^{30} + 9\,107\,567\tfrac{1}{4}\mu^{28} + 4\,374\,150\mu^{26}$$
$$- 5\,401\,545\tfrac{3}{4}\mu^{24} - 19\,734\,007\tfrac{1}{2}\mu^{22} - 31\,663\,835\tfrac{1}{4}\mu^{20} - 24\,921\,147\mu^{18}$$
$$+ 15\,503\,661\mu^{16} + 51\,659\,587\tfrac{1}{2}\mu^{14} - 31\,390\,220\tfrac{1}{4}\mu^{12} + 4\,480\,345\tfrac{4}{5}\mu^{10}$$
$$- 114\,043\tfrac{1}{2}\mu^{8}$$

$$\psi_{21} = \mu^{73} + 12\mu^{71} + 64\mu^{69} + 278\mu^{67} + 999\mu^{65} + 3\,182\mu^{63} + 9\,165\mu^{61} + 24\,306\mu^{59}$$
$$+ 60\,044\mu^{57} + 139\,116\mu^{55} + 303\,995\mu^{53} + 628\,456\mu^{51} + 1\,232\,166\mu^{49}$$
$$+ 2\,292\,792\mu^{47} + 4\,046\,141\mu^{45} + 6\,765\,535\mu^{43} + 10\,676\,044\mu^{41}$$
$$+ 15\,824\,846\mu^{39} + 21\,840\,760\mu^{37} + 27\,624\,314\mu^{35} + 31\,188\,812\mu^{33}$$
$$+ 29\,465\,072\mu^{31} + 18\,559\,819\mu^{29} - 4\,700\,234\mu^{27} - 41\,340\,065\mu^{25}$$
$$- 83\,441\,107\mu^{23} - 101\,586\,109\mu^{21} - 47\,879\,154\mu^{19} + 91\,306\,307\mu^{17}$$
$$+ 153\,554\,339\mu^{15} - 125\,973\,077\mu^{13} + 23\,835\,698\mu^{11} - 1\,007\,093\mu^{9}$$
$$+ 2\,428\tfrac{1}{7}\mu^{7}$$

References

Martin J L 1974 *Phase Transitions and Critical Phenomena*, eds C Domb and M S Green, vol 3 (London: Academic Press) chap 2

Sykes M F *et al* 1966 *J. Math. Phys.* **7** 1557–72

Sykes M F, Essam J W and Gaunt D S 1965 *J. Math. Phys.* **6** 283–98

Sykes M F, Gaunt D S, Essam J W and Hunter D L 1973a *J. Math. Phys.* **14** 1060–5

Sykes M F *et al* 1973b *J. Math Phys.* **14** 1066–70

—— 1973c *J. Math. Phys.* **14** 1071–4

—— 1973d *J. Phys.* A: *Math., Nucl. Gen.* **6** 1498–506

—— 1973e *J. Phys.* A: *Math., Nucl. Gen.* **6** 1507–16

Sykes M F and Watts M G 1975 *J. Phys.* A: *Math. Gen.* **8** 1469–79

Sykes M F, Watts M G and Gaunt D S 1975 *J. Phys.* A: *Math. Gen.* **8** 1441–7

Syozi I 1972 *Phase Transitions and Critical Phenomena*, eds C Domb and M S Green, vol 1 (London: Academic Press) chap 7